Structural Basis for the Interaction of a Vascular Endothelial Growth Factor Mimic Peptide Motif and Its Corresponding Receptors

Ricardo J. Giordano,[1,4] Cristiane D. Anobom,[2,4]
Marina Cardó-Vila,[1] Jorge Kalil,[3] Ana P. Valente,[2]
Renata Pasqualini,[1,*] Fabio C.L. Almeida,[2,*]
and Wadih Arap[1,4,*]
[1]The University of Texas
M.D. Anderson Cancer Center
Houston, Texas 77030
[2]National Center of Nuclear Magnetic Resonance
Institute of Medical Biochemistry
Federal University of Rio de Janeiro
Rio de Janeiro, RJ 21941-590
Brazil
[3]Heart Institute
University of São Paulo School of Medicine
São Paulo, SP 05403
Brazil

Summary

Vascular endothelial growth factor (VEGF) is central to the survival and development of the vascular and nervous systems. We screened phage display libraries and built a peptide-based ligand-receptor map of binding sites within the VEGF family. We then validated a cyclic peptide, CPQPRPLC, as a VEGF-mimic that binds specifically to neuropilin-1 and VEGF receptor-1. Here, we use NMR spectroscopy to understand the structural basis of the interaction between our mimic peptide and the VEGF receptors. We show that: (1) CPQPRPLC has multiple interactive conformations; (2) receptor binding is mediated by the motif Arg-Pro-Leu; and (3) the Pro residue within Arg-Pro-Leu participates in binding to neuropilin-1 but not to VEGF receptor-1, perhaps representing an evolutionary gain-of-function. Therefore, Arg-Pro-Leu is a differential ligand motif to VEGF receptors and a candidate peptidomimetic lead for VEGF pathway modulation.

Introduction

Vascular endothelial growth factor (VEGF) and its family members are key molecules in blood vessel formation [1–4]. These growth factors bind to two families of cell surface receptors: the tyrosine kinase receptors (VEGFR-1, VEGFR-2, and VEGFR-3) and the neuropilins (NRP-1 and NRP-2). VEGFR-1—a high-affinity receptor for VEGF, placental growth factor (PIGF), and VEGF-B—is essential for blood vessel formation [5], but its full biological role is still not entirely clear (reviewed in [4]). VEGFR-1 participates in tissue revascularization [6], receptor cross-activation [7], and monocyte-mediated arteriogenesis [8]. On the other hand, NRP-1 was first identified as a plexin/semaphorin receptor involved in neuron axon guidance, but was later shown to also be

a VEGF receptor; NRP-1 binds VEGF-B and PIGF, and has an essential role in blood vessel formation [9, 10]. Some of the similarities between the vascular and nervous systems (i.e., branched, ramified networks) are not merely coincidental, because they appear to share molecular mechanisms for differentiation and patterning formation [11–13]. Recently, it became clear that VEGF and its receptors are essential not only for blood vessel formation but also in the nervous system [14, 15]. In fact, VEGF is a pleiotropic growth factor with functions such as neuroprotection, learning and memory, glial proliferation, and even neurogenesis itself [15, 16].

In previous work, we selected and isolated a cyclic peptide (sequence CPQPRPLC) from a phage display random peptide library on VEGF-stimulated endothelial cells; we also validated CPQPRPLC as a VEGF receptor-ligand specifically targeting VEGFR-1 and NRP-1 [17]. CPQPRPLC contains two overlapping binding motifs [18]: PRPLC (an NRP-1 binding site within VEGF-B$_{167}$) and PQPR (embedded within a 12-residue NRP-1 binding site within VEGF-B$_{186}$). Thus, in essence, CPQPRPLC is a chimera between overlapping binding sites in different VEGF-B isoforms. Of note, we observed marked differences in the relative inhibitory effect (concentration producing half-maximum inhibition of effect [IC$_{50}$]) when the synthetic peptide CPQPRPLC was used to compete for phage binding to either VEGF receptor [17]. Therefore, while the molecular basis for the binding remains elusive, we reasoned that CPQPRPLC interacts with its corresponding VEGF receptors differentially. Here, we use nuclear magnetic resonance (NMR) spectroscopy-based screening methodology to elucidate the structural requirements for binding of CPQPRPLC to VEGFR-1 and to NRP-1. We show that the differential binding of CPQPRPLC to both VEGF receptors relies on residues within the motif Arg-Pro-Leu (RPL); this tripeptide may prove useful as a lead for the design and development of drugs that modulate VEGF pathways.

Results

The VEGF-like Peptide CPQPRPLC Has Multiple Conformations

To study the interaction of CPQPRPLC with its corresponding VEGF receptors, we first set out to understand the behavior of the synthetic peptide in solution. For an exclusive peptide conformation, only eight resonance lines would be expected in the amide region of a one-dimensional proton NMR spectrum (1D-^{1}H-NMR): five amide backbones, two Gln side chains, and one Arg side chain. Instead, NMR spectrum analysis of CPQPRPLC revealed 16 resonances at 45ºC, 14 resonances at 25ºC, and 12 resonances at 0ºC, indicating the presence of multiple peptide conformations in aqueous solution (Figure 1). Proline *trans*-isomers seemed to be favored at lower temperatures and, indeed, the residue Pro4 was found only in *trans*-conformation below 5ºC. While virtually all residues showed multiple conformers, the highest degree of structural variability

*Correspondence: warap@mdanderson.org (W.A.), falmeida@cnrmn.bioqmed.ufrj.br (F.C.L.A.), rpasqual@mdanderson.org (R.P.)
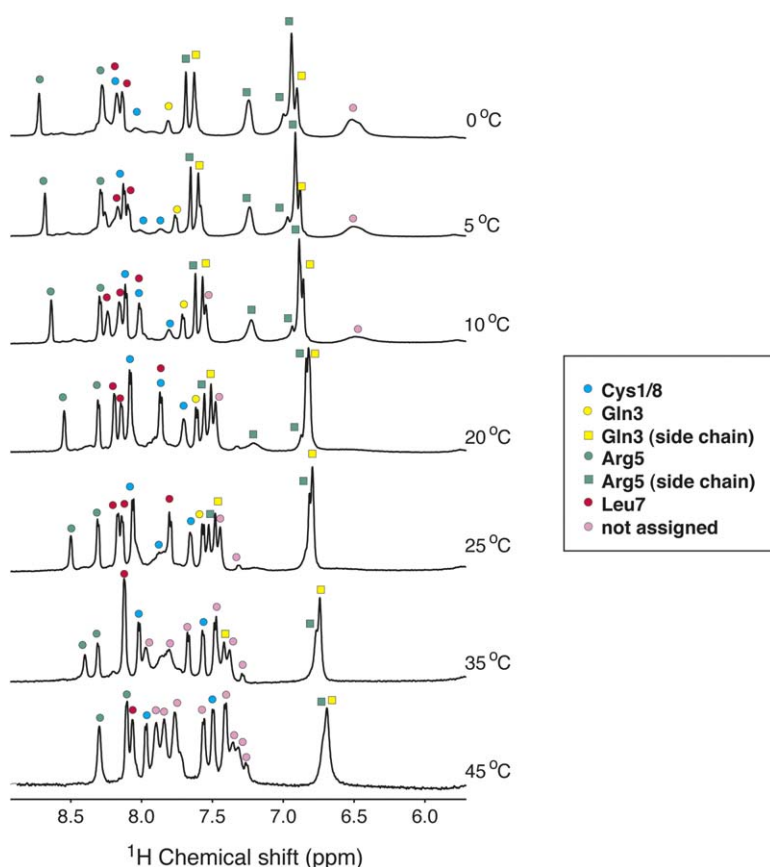[4]These authors contributed equally to this work.

Figure 1. The Synthetic Peptide CPQPRPLC Has Multiple Conformers

One-dimensional ^{1}H-NMR spectra of the synthetic peptide (amide region) performed at decreasing temperatures are shown. Peaks are color-coded. Circles represent amide resonances and squares represent side-chain resonances.

was found within the Leu7-Cys8-Cys1-Pro2 region, likely induced by *trans*-isomerization of the disulfide bond, Pro residues, or both. Although such conformational variability tended to decrease toward lower temperatures, ultimately, a unique lowest-energy conformer was not observed (Figure 1). Conformational variability of the CPQPRPLC peptide persisted in other nonaqueous organic solvents, such as dimethylsulfoxide (DMSO) or trifluorethanol (TFE).

The Arginine and Leucine Residues of CPQPRPLC Mediate Binding of the Peptide Conformers to VEGF Receptors

The conformational variability displayed by the peptide notwithstanding, we sought to determine the residues primarily responsible for the binding of CPQPRPLC to VEGFR-1 and to NRP-1. Typically, low-affinity peptide-receptor interactions (i.e., micromolar range) are observed in NMR spectra as average resonances between free and bound forms; thus, if the binding equilibrium is in fast exchange regime (i.e., microseconds), the NMR parameters will reflect the bound state even if an excess of free peptide is used [19–21]. Therefore, we performed binding experiments with a large molar excess of CPQPRPLC peptide to determine chemical shift changes from 1D-^{1}H-NMR at 25°C between the synthetic peptide and the recombinant receptors, VEGFR-1 or NRP-1, in solution. Given the multiple conformers and consequent overlapping of peaks, we placed emphasis on the analysis of the amide resonances. When CPQPRPLC was incubated with either VEGFR-1 or

NRP-1, only the peptide resonance lines were observed; moreover, resonance lines of residues interacting with each receptor were shifted relative to the spectrum of CPQPRPLC alone (Figures 2 and see Figure S1 in the Supplemental Data available with this article online). Different binding attributes were noted for each peptide-receptor interaction: VEGFR-1 induced chemical shift changes in CPQPRPLC resonance lines corresponding to Arg5 and Leu7 residues (Figure 2A). Notably, all resonance lines corresponding to these residues changed position. These data indicate that Arg5 and Leu7 are the two key residues involved in the binding of the CPQPRPLC to VEGFR-1. In addition to Arg5 and Leu7, NRP-1 induced chemical shift changes in resonance lines corresponding to Gln3 and Cys1/8 and, again, several resonances corresponding to the amide hydrogen of the same residue shifted (Figure 2B). The fact that different bands corresponding to the same residue changed position upon receptor binding suggests that CPQPRPLC binding is most likely independent of a unique peptide conformation, since the timescale of binding and of the exchange processes are more than two orders of magnitude different. Two different timescales occur during the binding of CPQPRPLC to the VEGF receptors. The first one is the conformational exchange among the different CPQPRPLC conformers. Because such conformational exchange results in different spin systems (more then one resonance for the same residue), this timescale is in the tens of milliseconds or slower. The second timescale is that associated with the binding of the peptide to both VEGFR-1 and
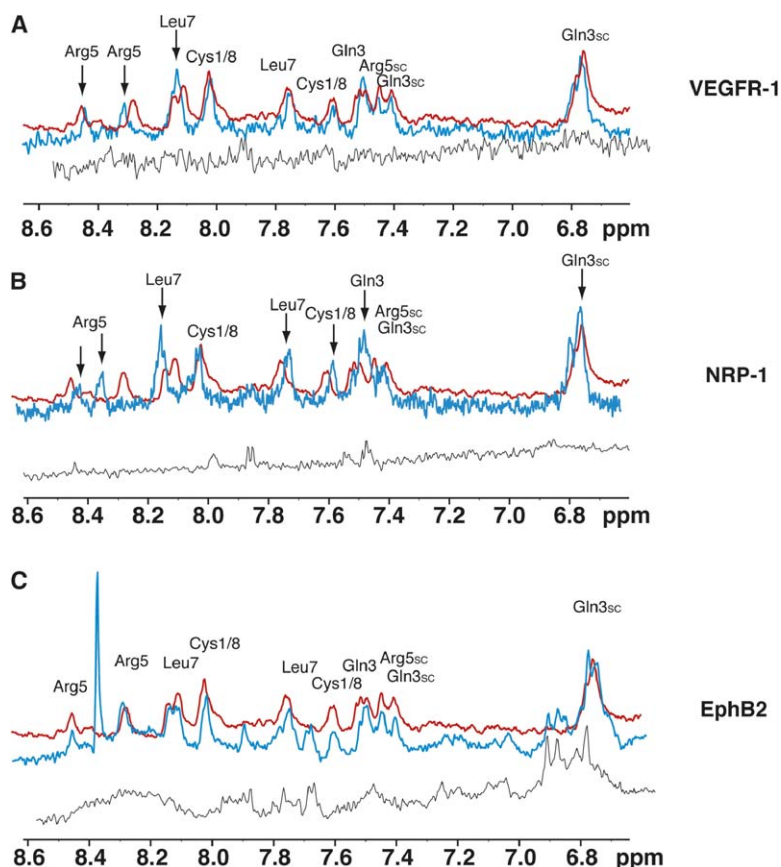
Figure 2. Identification of Specific CPQPRPLC Residues Interacting with VEGF Receptors

Amide region of the one-dimensional ^{1}H-NMR spectra of CPQPRPLC free (red lines) and in the presence of the indicated receptor (blue lines) are shown; CPQPRPLC peptide concentration were 140 µM (A), 280 µM (B), and 140 µM (C); black lines represent the spectra of the receptors alone under identical experimental conditions. In each case, arrows indicate resonances that shifted in the presence of the receptor. Receptor concentrations were: 2 µM of VEGFR-1 (A), 1 µM of NRP-1 (B), and 2 µM of ephrin-B2 (EphB2) (C).

NRP-1 receptors. In this case, the timescale is in a fast exchange regime (most likely in the microsecond range), resulting in single resonances and line shifts when in the presence of large excess of ligands (peptides). Particularly, in the case of CPQPRPLC, several resonances corresponding to the amide hydrogen of the same residue shifted upon binding to both VEGFR-1 and NRP-1, indicating that more than one conformer of the peptide interact with the receptors. Our conclusions, however, do not imply that there is more then one conformation of the peptide in the bound state. In contrast, an unrelated membrane receptor, Ephrin-B2 (EphB2), used as a negative control did not induce detectable chemical shift changes in CPQPRPLC resonance lines (Figure 2C). Taken together, these data indicate that the interaction between CPQPRPLC and its corresponding VEGF receptors (1) is not dependent on a unique conformation of the peptide, and (2) it is most likely mediated by the residues Arg5 and Leu7. Given that the motif RPL contains both of these residues within CPQPRPLC, we next set out to determine whether this motif would represent a minimal peptide binding site for receptor interaction.

Deconstruction of CPQPRPLC into Overlapping Tripeptide Motifs Reveals the Structural Basis for the Peptide-Receptor Interaction
We next used small CPQPRPLC-derived motifs to circumvent the ambiguities preventing a full analysis of side-chain interactions and to resolve the possible roles of Gln3 and Pro6 residues in differentiating ligand-

receptor binding of CPQPRPLC to NRP-1 versus VEGFR-1. Toward that goal, we designed, synthesized, and analyzed the binding of two overlapping tripeptide motifs, Gln-Pro-Arg (QPR) and RPL to VEGFR-1 and to NRP-1. We hypothesized that the motif RPL might suffice for mediating an interaction with either NRP-1 or VEGFR-1; RPL analysis would also allow us to evaluate the role of Pro6 in differentiating the binding of CPQPRPLC to NRP-1 versus VEGFR-1. TOCSY and NOESY experiments were carried out and the resonances of each tripeptide were assigned either free in solution or in the presence of each individual receptor (Table S1). Side-chain chemical shift changes were observed with both receptors for the motif RPL. Indeed, all resonances in RPL and QPR were analyzed unambiguously in the presence of VEGFR-1 or NRP-1. The interaction of RPL with VEGFR-1 or NRP-1 caused chemical shift changes of amide and side-chain hydrogen atoms of Arg1 and Leu3 of RPL (Figure 3 and Table 1). In the case of VEGFR-1, no such changes associated with the Pro hydrogen atoms were detected. These experiments show that Arg and Leu are the primary residues that interact with both receptors. However, the interaction of RPL with NRP-1 also involves the participation of the Pro residue side chain, as evidenced by the 8.8 Hz chemical shift of Pro.HB hydrogen and the 4.4 Hz chemical shift change of Pro.HG2 (Figure 3 and Table 1). In contrast, no changes of this magnitude were detected for the motif QPR, except for a much smaller (2.2 Hz) shift of Arg3 amide resonance in the presence of NRP-1 (Figure S3), making it unlikely that the motif QPR
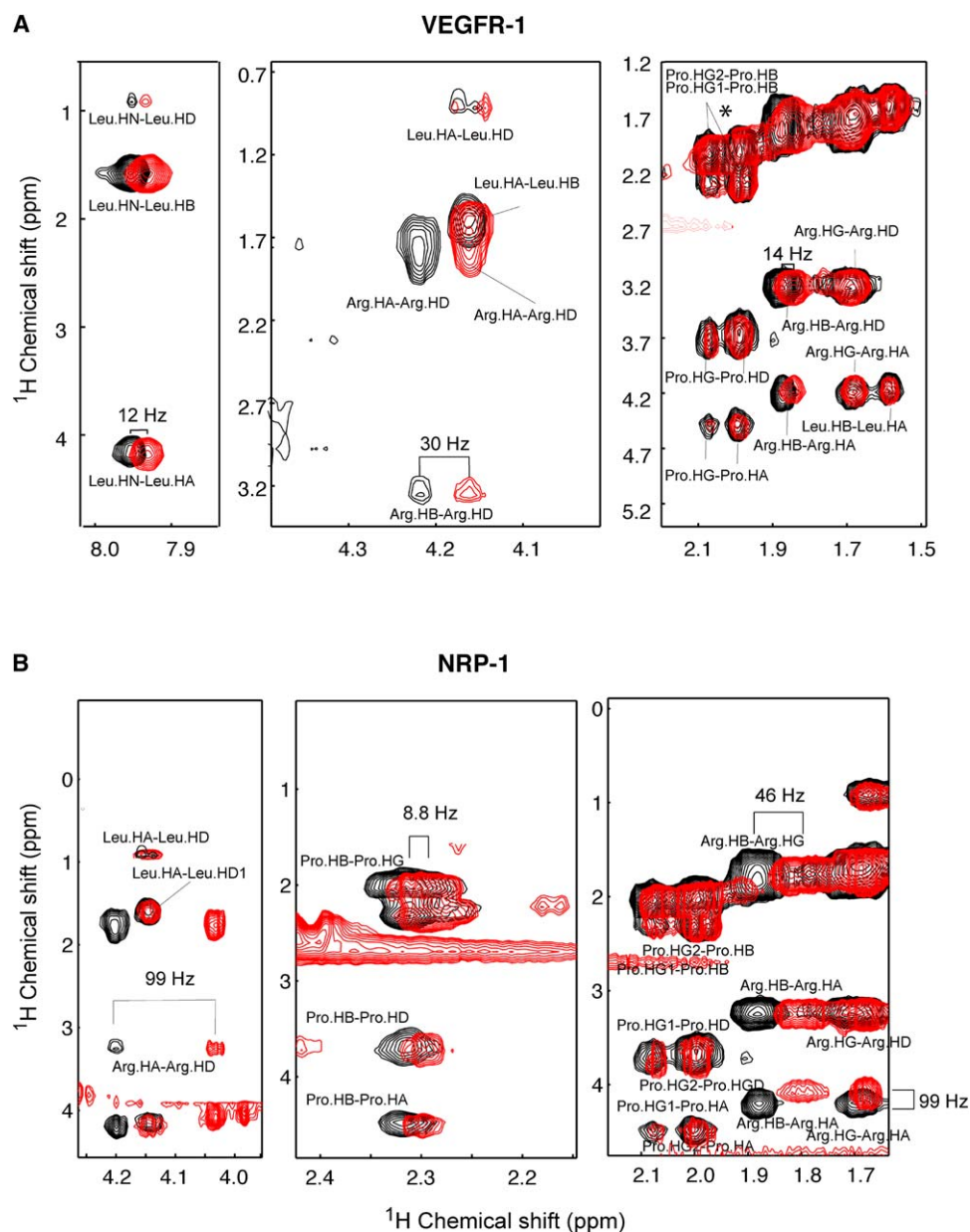
A

VEGFR-1

B

NRP-1

Figure 3. Chemical Shift Changes Induced on the Arg-Pro-Leu Motif by Binding to VEGFR-1 and to NRP-1

Two-dimensional TOCSY spectra of Arg-Pro-Leu (800 μM) alone (black) or in the presence of VEGF receptors (red) are shown. Either 2 μM VEGFR1 (A) or 1 μM NRP-1 (B) were used. Chemical shift changes are indicated. Asterisks point to the lack of detectable chemical shift changes in the hydrogen atoms of the Pro residue in the presence of VEGFR-1 (upper right, [A]) relative to the 8.8 Hz chemical shift change observed in the presence of NRP-1 (middle panel, [B]).

interacts with NRP-1. Together, these results show that the motif RPL mediates the interaction to both VEGF receptors within CPQPRPLC, but the Pro6 residue participates only in the binding to NRP-1. Of note, receptor-ligand interactions are dose-dependent and, in our case, the NMR parameter (chemical shift changes) should vary with the peptide concentration. If the fast exchange regime is reached, chemical shift perturbations should become smaller with increasing concentrations of the peptide. In the case of CPQPRPLC peptide, we observed little effect of the peptide concentration upon the chemical shift changes (Figure S1). However, due to the narrow range of molar concentrations used

(60–280 μM) in the experimental design (in order to avoid peptide oligomerization), no conclusions could be reached. It is also relevant that peptide oligomers by themselves may induce changes in the peptide lines, making it sometimes difficult to distinguish from the changes induced by receptor binding. This was not a concern for the smaller motifs (RPL and QPR), since they could be used in a wider molar concentration range of (40–800 μM) without noticeable oligomerization. In the case of the RPL motif, we did observe a clear concentration-dependent effect upon the chemical shift changes (Figure S2). The observed parameter, chemical shift perturbation, did not go back to zero but, as

Table 1. Chemical Shift Changes for the RPL Interaction with VEGFR-1 or NRP-1

Residues	$\Delta\delta$ (RPL$_{free}$ − RPL$_{bound}$) VEGFR-1 (Hz)	$\Delta\delta$ (RPL$_{free}$ − RPL$_{bound}$) NRP-1 (Hz)
Arg.HA	30	99
Arg.HB	14	46
Arg.HG	2.5	6.6
Arg.HD	3.0	6.6
Pro.HB	0.0	8.8
Pro.HG1	0.0	2.0
Pro.HG2	0.0	4.4
Leu.HN	12	11
Leu.HA	0.0	0.0
Leu.HB	0.0	0.0
Leu.HG	0.0	ND[a]
Leu.HD1	1.3	2.2
Leu.HD2	1.1	2.2

Differences in chemical shift change were determined in free RPL (800 μM) and in the presence of VEGFR-1 (2 μM) or NRP-1 (1 μM) and calculated from 2D-TOCSY. Pro.HA was not determined due to overlap with water. Labile resonances (Arg.HN, HE, and HH) were not detected due to fast solvent exchange.
[a] ND, not determined due to overlapping of peaks.

Table 2. Individual T_1 Values and Differences between Free and Bound RPL

Hydrogen	RPL Bound, ms (SEM)	RPL Free, ms (SEM)	ΔT_1[a], ms (SEM)
Arg.HB	455 (15.6)	379 (7.80)	76.0 (23.4)[b]
Arg.HG	653 (50.7)	549 (20.9)	104 (71.6)
Arg.HD	560 (39.8)	536 (17.2)	24.0 (57.0)
Pro.HB	671 (30.9)	679 (55.9)	8.00 (86.8)
Pro.HG2	680 (25.2)	666 (26.9)	14.0 (52.1)
Leu.HN	459 (11.9)	519 (18.9)	−60.0 (30.8)[b]
Leu.HB	724 (34.0)	590 (27.8)	134 (61.8)[b]
Leu.HB	514 (9.00)	450 (19.2)	64.0 (28.2)[b]
Leu.HD	899 (67.4)	630 (4.30)	269 (71.7)[b]
Leu.HD	752 (61.7)	668 (8.64)	84 (70.3)

Longitudinal relaxation changes (ΔT_1) of RPL peptide hydrogen, free or in the presence of VEGFR-1. Leu.HA, Arg.HA, and Pro.HG1 were not determined due to receptor overlapping. Pro.HA was not determined due to overlap with water.
[a] ΔT_1 represents difference between bound and free states.
[b] ΔT_1 greater than 2-fold SEM.

expected, decreased with the increasing concentration of free peptide. Similar experiments performed with the noninteractive QPR motif showed no effect upon the resonance lines (Figure S3).

Finally, to confirm that the Pro6 residue of CPQPRPLC is not necessary for VEGFR-1 binding (as it is for NRP-1), we used another NMR-based screening method: the involvement of the RPL side-chain interaction with VEGFR-1 was analyzed by determining longitudinal relaxation time (T_1) changes. It is established that T_1 varies depending on differences in the effective correlation time, which is affected by the molecule tumbling rates, local dynamics, and cross-relaxation [21]; as a result, upon peptide-receptor binding, distinct tumbling rates between the free and bound peptides are induced (by the large difference in molecular weights between the free peptide and the corresponding receptor). However, the close proximity of residue side chains to the receptor also changes T_1, allowing the mapping

of atoms directly involved in the interaction. T_1 was measured with a large molar excess of RPL in the presence of VEGFR-1. Individual T_1 values and differences in T_1 between the free and bound peptides (ΔT_1) were determined (Table 2) and used for mapping (Figure 4). ΔT_1 values were greater for hydrogen atoms in the Arg and Leu side chains that either had decreased local motion, or underwent cross-relaxation with the receptor, or both. No changes in T_1 were observed for Pro hydrogen atoms. These longitudinal relaxation data are consistent with the chemical shift mapping results (Figure 4) and indicate that Leu methyl groups are involved in the VEGFR-1 interaction. These data further support the contention that the Pro residue of CPQPRPLC is not required for the interaction with VEGFR-1.

Discussion

An application of phage display screenings is to map functional protein interacting sites that may serve as leads for rational drug design. Over the past few years, we have identified peptide ligands for biochemical
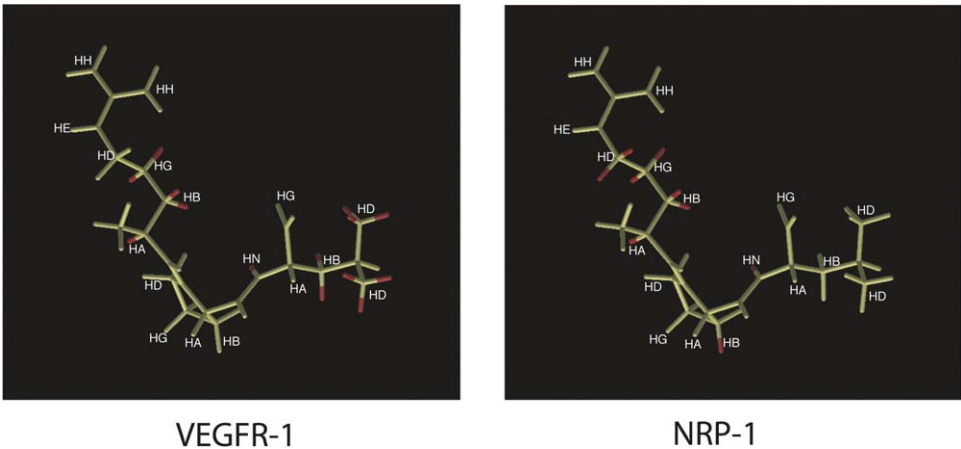

VEGFR-1

NRP-1

Figure 4. Representation of the Atoms within the Motif Arg-Pro-Leu Affected by Receptor Binding to VEGFR-1 or NRP-1

Hydrogen atoms displaying changes in chemical shift or cross-relaxation time (T_1) caused by the presence of each receptor are indicated in red.

markers of angiogenic blood vessels, including motifs binding to cell adhesion molecules [23], proteoglycans [24], membrane-bound proteases [25, 26], and growth factor receptors [17, 27]. By screening phage display libraries on VEGF-stimulated human endothelial cells, we have discovered the VEGF-like sequence CPQPRPLC; we have also shown that this cyclic peptide binds specifically to VEGFR-1 and to NRP-1 [17]. In this work, we used NMR to gain mechanistic insight into the structural attributes of this VEGF receptor-ligand interaction.

We initially analyzed the structural behavior of CPQPRPLC by 1D-^{1}H-NMR. We found that the peptide has many conformations, regardless of chemical environment (aqueous and organic solvents) or temperature (from 0°C to 45°C). Such structural variability is most likely secondary to the cis-/trans-isomerization of either the disulfide bond or the three Pro residues (or both). Thus, while cyclic peptides are often referred to as "conformationally constrained," these results illustrate that—in the absence of structural data—this assumption must be made with caution.

Because of the structural diversity of CPQPRPLC, we used chemical shift change analysis of the backbone hydrogen atoms to identify the key residues mediating the interaction between the VEGF-like peptide and its VEGF receptors. We found that the residues Arg5 and Leu7 are critical to the binding to both VEGF receptors studied. These findings indicate that, regardless of the intrinsic conformational variability of the peptide, the binding mechanism is not dependent on a unique conformation of the peptide, and suggest that residues within the motif RPL are central for interactions with both VEGF receptors. However, if this is so, why would the IC$_{50}$ of the synthetic peptide CPQPRPLC for CPQPRPLC-phage binding to NRP-1 be 100-fold higher [17] than that for binding to VEGFR-1? To address this question, we analyzed the interaction of two CPQPRPLC-derived overlapping tripeptides (QPR and RPL) with the NRP-1 and VEGFR-1. Essentially, the multi-conformational nature of the CPQPRPLC peptide created several ambiguities in its ^{1}H-NMR spectrum, which prevented a more detailed analysis of the binding of the peptide to its corresponding VEGF receptors. Thus, deconstruction of the peptide CPQPRPLC into two linear tripeptide motifs was the approach used to unequivocally show that the tripeptide RPL is indeed a receptor binding motif, and to fully understand the involvement of each residue in the ligand binding process. In particular, we show that the Pro residue within the RPL motif (Pro6) participates in binding to NRP-1 but not to VEGFR-1; thus, we propose that the involvement of Pro6 strengthens the interaction of the peptide with NRP-1 and induces changes in the backbone of CPQPRPLC. These data are consistent with the larger chemical shift changes observed upon binding of CPQPRPLC (or RPL) to NRP-1, and may also explain the chemical shift changes in the residues Gln3 and Cys1/8 of CPQPRPLC during its interaction with NRP-1.

Keeping in mind that CPQPRPLC was originally identified as a sequence with similarity to human VEGF-B isoforms [17], we next compared the protein sequences encoded by VEGF-B genes from different species. Arg and Leu residues are conserved cross-species from rodents to humans, but the Pro residue is not. Specifically, the Pro residue within the motif RPL is not present in mice (Arg-Ile-Leu) or rats (Arg-Thr-Leu). Whether the presence of Pro in this binding site represents an evolutionary gain-of-function remains an open question; however, one might speculate that Ile or Thr side chains may interact with NRP-1 through their methyl or ethyl groups, perhaps compensating for the absence of a Pro ring. Although the binding of human VEGF-B to NRP-1 has been documented [18], no information is as yet available on whether rodent VEGF-B binds to NRP-1, and if so, with what relative affinity compared to human VEGF-B. Thus, at this point, the functional significance of this finding, while provocative, remains unknown. However, given that the structure of the heparin binding domain of VEGF has been solved [28], we modeled the location and receptor accessibility of RPL in the native VEGF-B molecule (Figure 5A). Analysis of this molecular model suggests that the motif RPL belongs to a distinct binding site, outside of the heparin binding pocket. Of note, eight charged residues (Arg and Lys) are conserved and may form the basic groove responsible for heparin binding interactions (Figures 5B and 5C). This model is consistent with RPL being exposed and accessible for ligand-receptor binding to NRP-1 and to VEGFR-1.

In summary, the work presented here establishes CPQPRPLC as a bona fide ligand peptide to VEGF receptors. Despite its conformational variability, we determined that the tripeptide RPL is a critical motif for receptor binding to NRP-1 and to VEGFR-1, and that the Pro residue within RPL may account for the difference observed in binding efficiency to either receptor. Since drugs that interfere with VEGF pathways have shown great promise in clinical trials [1–3, 29, 30], peptidomimetics based on these structural insights may prove useful for rational drug design.

Significance

In theory, phage display and NMR spectroscopy are complementary technologies to study protein-protein interactions. However, while conceptually appealing, serial integration of phage display to NMR has been hampered by technical challenges (such as, for example, the possibility of multiple conformations arising from a small peptide ligand). Recently, it became clear that angiogenesis and neuronal development share molecular mechanisms for specification, differentiation, and patterning formation. Given that VEGF and its receptors participate in both systems, understanding such ligand-receptor interactions is essential for the design of VEGF-targeted therapies. Here, as a proof-of-concept, we used NMR to determine the structural basis for the differential binding of the peptide CPQPRPLC (selected from a random phage display library) to its corresponding VEGF receptors. We analyzed chemical shift changes induced by each receptor upon the peptide resonances to pinpoint the key residues responsible for the interaction with VEGFR-1 and NRP-1. We showed that the tripeptide motif Arg-Pro-Leu contained within the peptide is sufficient for binding to both receptors, but that Pro6 is a differential residue that participates only in binding
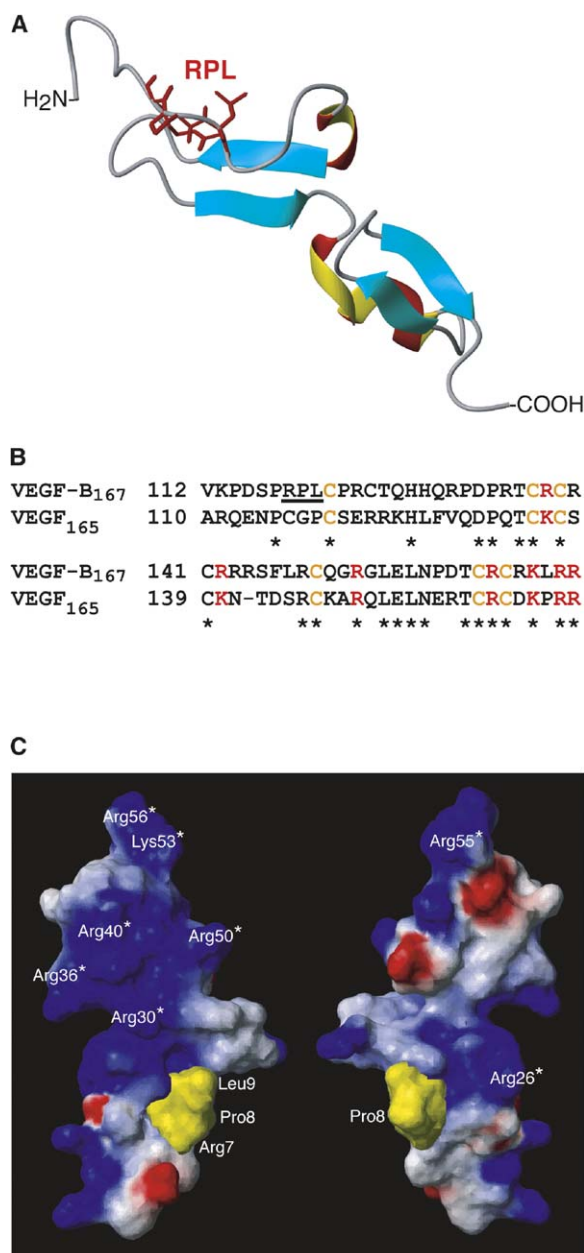
Figure 5. Molecular Modeling of the Heparin Binding Domain in VEGF-B$_{167}$

(A) Ribbon model of the VEGF-B$_{167}$ heparin binding domain (HBD). Side-chain residues of the tripeptide Arg-Pro-Leu within the native VEGF-B$_{167}$ molecule are represented in red.

(B) Color-coded sequence alignment of human HBD of both VEGF-B$_{167}$ and VEGF$_{165}$: basic residues (Arg or Lys; red) and Cys (orange) are indicated; the motif Arg-Pro-Leu is highlighted.

(C) Solvent-accessible molecular interface of the VEGF-B$_{167}$ HBD model, color-coded to represent electrostatic surface potential: red, −10 kT; white, 0 kT; and blue, 10 kT. The two views are related by a 180° rotation around the vertical axis. Yellow indicates the Arg-Pro-Leu motif. Asterisks represent conserved Arg and Lys residues. Moreover, all but a single residue are in a favorable region of the Rammachandran plot; however, the exception, Lys 2, is contained within the very flexible N-terminal region (residues 1–9), as determined by ^{15}N heteronuclear NOE of the VEGF$_{165}$ HBD [28].

to NRP-1. Thus, the work presented here not only defines Arg-Pro-Leu as a new VEGF receptor binding motif, but also illustrates how the screening of phage display peptide libraries and NMR-based technology can synergize to translate targeting peptide-protein interactions into potential drug delivery tools.

Experimental Procedures

Reagents

Synthetic peptides were generated by Merrifield synthesis to over 95% purity in solid-phase F-MOC (AnaSpec, San Jose, CA). A standard cyclization protocol was used: exposure to air followed by cysteine oxidation in ammonium bicarbonate buffer, pH 8. The cyclization and the absence of disulfide-bonded oligomers of CPQPRPLC were confirmed by mass spectrometry. Further confirmation was obtained by reduction and re-formation of the disulfide bond under controlled conditions. The postrefolding NMR spectrum was found to be identical to the original spectrum. Peptides were solubilized in phosphate-buffered saline (PBS) buffer (136 mM NaCl, 2 mM KCl, 8 mM Na$_2$HPO$_4$, and 1 mM KH$_2$PO$_4$) at pH 7.2 and 10% D$_2$O (99.9%; Isotec, Inc., Miamisburg, OH) for lock purposes. Experiments were performed in aqueous solution (PBS) unless otherwise specified; when indicated, additional peptide spectra were also obtained by increasing concentrations of the organic solvents DMSO (from 0% to 100%) or TFE (from 0% to 60%) in water. The recombinant receptors VEGFR-1, NRP-1, and EphB2 were purchased from R&D Systems (Minneapolis, MN).

NMR Spectroscopy

NMR experiments were generated on a 600 MHz spectrometer (Bruker Avance DRX). Chemical shift assignment was accomplished by using CPQPRPLC (1 mM), RPL (500 μM), and QPR (400 μM) in PBS (Table S1). One-dimensional spectra were acquired at temperatures ranging from 0°C to 45°C and were collected with 4096 data points in F2, with 256 transients. NOESY spectra [31] were acquired by setting a 200 ms mixing time. Spectra were collected with 400 data points in F1 and 4096 data points in F2, with 80 transients. Water suppression was achieved by using the WATERGATE technique [32]. TOCSY spectra (spin-lock time, 80 ms) were acquired by using the MLEV-17 pulse sequence [33]. The spectrum was collected with 400 data points in F1 and 4096 data points in F2, with 32 transients. These experiments were performed at 5°C.

Analysis of Peptide-Receptor Interactions

A series of one-dimensional ^{1}H-NMR spectra of peptides in the presence of the VEGF receptors or control proteins was obtained at 25°C. The recombinant receptors used in this work (VEGFR-1 and NRP-1) were obtained as fusion proteins to the Fc portion of the human IgG$_1$ domain Pro$_{100}$-Lys$_{330}$. Thus, to ensure that any observed chemical shift changes were specific to the receptor binding domain (and not to the Fc portion), experiments were repeated under the same conditions by using an unrelated membrane receptor (EphB2) containing the same fusion protein domain. Unless otherwise specified, EphB2 served as a negative control receptor because it is a membrane bound vascular receptor with a similar molecular weight. Receptor concentrations used were 2 μM for VEGFR-1, 1 μM for NRP-1, and 2 μM for EphB2. Synthetic peptides were used in increasing concentrations, from 10 to 800 μM. Pilot experiments revealed that the three synthetic peptides were in their respective monomeric states under the experimental conditions used. Specifically, the ^{1}H-NMR spectra with increasing concentration of each individual peptide were analyzed and no significant band shifts were observed (up to 1 mM). Only in the case of CPQPRPLC were very small shifts observed (above 400 μM), but they did not prevent the correct assignment of the peptide. To further minimize the possibility of peptide oligo-/multimerization, we kept the concentration of CPQPRPLC under 400 μM in experiments on binding to VEGFR-1 and to NRP-1. For refinement of the analysis of peptide-receptor interaction, TOCSY and NOESY were performed by using 2 μM VEGFR-1, 1 μM NRP-1, and 800 μM of each peptide. One-dimensional spectra were collected with 4096 data points in F2, with 16 to 10240 transients. Sodium 2,2-dimethyl-2-silapentane-5-sufonate

(DSS) (50–100 μM) served as a reference standard for precise spectra overlapping and comparison.

Longitudinal Relaxation Time Measurements

T_1 experiments were performed by inversion-recovery [22] using RPL (400 μM) in the presence and absence of VEGFR-1 (10 μM). Spectra were collected with 8192 data points in F2, with 1024 scans. T_1 relaxation times in the pulse sequence varied from 100 ms to 4 s (n = 11 points). The intensity of each peak in the spectrum was measured and plotted as a function of the T_1 relaxation time.

Molecular Modeling

Homology modeling was done by fitting the primary sequence of the human VEGF-B$_{167}$ C terminus (residues 112–167; GenBank no. AAL79000) to the three-dimensional structure of VEGF (http://www.rcsb.org/pdb/; PDB accession codes 2VGH and 1VGH; [27]). Swiss-Model [34], a homology modeling server Web interface (http://www.expasy.ch/swissmod/), was used for the structural fitting. Refinements of the model, such as the search for side-chain rotamers, the reconstruction of loops, and the energy minimization, were done through Swiss-PdbViewer (SPDBV) [34].

Supplemental Data

Supplemental Figures S1–S3 and Table S1 are available online at http://www.chembiol.com/cgi/content/full/12/10/1075/DC1/.

References

1. Folkman, J., and Kalluri, R. (2004). Cancer without disease. Nature *427*, 787.
2. Carmeliet, P. (2003). Angiogenesis in health and disease. Nat. Med. *9*, 653–660.
3. Folkman, J. (2003). Angiogenesis inhibitors: a new class of drugs. Cancer Biol. Ther. *2* (4 Suppl 1), S127–S133.
4. Ferrara, N., Gerber, H.P., and LeCouter, J. (2003). The biology of VEGF and its receptors. Nat. Med. *9*, 669–676.
5. Fong, G.H., Rossant, J., Gertsenstein, M., and Breitman, M.L. (1995). Role of the Flt-1 receptor tyrosine kinase in regulating the assembly of vascular endothelium. Nature *376*, 66–70.
6. Luttun, A., Tjwa, M., Moons, L., Wu, Y., Angelillo-Scherrer, A., Liao, F., Nagy, J.A., Hooper, A., Priller, J., De Klerck, B., et al. (2002). Revascularization of ischemic tissues by PlGF treatment, and inhibition of tumor angiogenesis, arthritis and atherosclerosis by anti-Flt1. Nat. Med. *8*, 831–840.
7. Autiero, M., Waltenberger, J., Communi, D., Kranz, A., Moons, L., Lambrechts, D., Kroll, J., Plaisance, S., De Mol, M., Bono, F., et al. (2003). Role of PlGF in the intra- and intermolecular cross talk between the VEGF receptors Flt1 and Flk1. Nat. Med. *9*, 936–943.
8. Pipp, F., Heil, M., Issbrucker, K., Ziegelhoeffer, T., Martin, S., van den Heuvel, J., Weich, H., Fernandez, B., Golomb, G., Carmeliet, P., et al. (2003). VEGFR-1-selective VEGF homologue PlGF is arteriogenic: evidence for a monocyte-mediated mechanism. Circ. Res. *92*, 378–385.
9. Kawasaki, T., Kitsukawa, T., Bekku, Y., Matsuda, Y., Sanbo, M., Yagi, T., and Fujisawa, H. (1999). A requirement for neuropilin-1 in embryonic vessel formation. Development *126*, 4895–4902.
10. Soker, S., Miao, H.Q., Nomi, M., Takashima, S., and Klagsbrun, M. (2002). VEGF$_{165}$ mediates formation of complexes containing VEGFR-2 and neuropilin-1 that enhance VEGF$_{165}$-receptor binding. J. Cell. Biochem. *85*, 357–368.
11. Weinstein, B.M. (2005). Vessels and nerves: marching to the same tune. Cell *120*, 299–302.
12. Vogel, G. (2005). Developmental biology: the unexpected brains behind blood vessel growth. Science *307*, 665–667.
13. Eichmann, A., Le Noble, F., Autiero, M., and Carmeliet, P. (2005). Guidance of vascular and neural network formation. Curr. Opin. Neurobiol. *15*, 108–115.
14. Yasuhara, T., Shingo, T., and Date, I. (2004). The potential role of vascular endothelial growth factor in the central nervous system. Rev. Neurosci. *15*, 293–307.
15. Jin, K., Zhu, Y., Sun, Y., Mao, X.O., Xie, L., and Greenberg, D.A. (2002). Vascular endothelial growth factor (VEGF) stimulates neurogenesis in vitro and in vivo. Proc. Natl. Acad. Sci. USA *99*, 11946–11950.
16. Cao, L., Jiao, X., Zuzga, D.S., Liu, Y., Fong, D.M., Young, D., and During, M.J. (2004). VEGF links hippocampal activity with neurogenesis, learning and memory. Nat. Genet. *36*, 827–835.
17. Giordano, R.J., Cardó-Vila, M., Lahdenranta, J., Pasqualini, R., and Arap, W. (2001). Biopanning and rapid analysis of selective interactive ligands. Nat. Med. *7*, 1249–1253.
18. Makinen, T., Olofsson, B., Karpanen, T., Hellman, U., Soker, S., Klagsbrun, M., Eriksson, U., and Alitalo, K. (1999). Differential binding of vascular endothelial growth factor B splice and proteolytic isoforms to neuropilin-1. J. Biol. Chem. *274*, 21217–21222.
19. Stockman, B.J., and Dalvit, C. (2002). NMR screening techniques in drug discovery and drug design. Prog. Nucl. Magn. Reson. *41*, 187–231.
20. Cooke, R.M. (1996). Protein-ligand interaction: examples in drug design. In NMR in Drug Design, D.J. Craik, ed. (New York: CRC Press), p. 245–274.
21. Pires, J.R., Taha-Nejad, F., Toepert, F., Ast, T., Hoffmuller, U., Schneider-Mergener, J., Kuhne, R., Macias, M.J., and Oschkinat, H. (2001). Solution structures of the YAP65 WW domain and the variant L30 K in complex with the peptides GTPPPPYTVG, N-(n-octyl)-GPPPY and PLPPY and the application of peptide libraries reveal a minimal binding epitope. J. Mol. Biol. *314*, 1147–1156.
22. Abragam, A. (1961). Principles of nuclear magnetism. In International series of monographs on physics, vol. 32 (Oxford: Oxford Science Publications, Clarendon Press), p. 264–353.
23. Pasqualini, R., Koivunen, E., and Ruoslahti, E. (1997). Alpha v integrins as receptors for tumor targeting by circulating ligands. Nat. Biotechnol. *15*, 542–546.
24. Burg, M.A., Pasqualini, R., Arap, W., Ruoslahti, E., and Stallcup, W.B. (1999). NG2 proteoglycan-binding peptides target tumor neovasculature. Cancer Res. *59*, 2869–2874.
25. Pasqualini, R., Koivunen, E., Kain, R., Lahdenranta, J., Sakamoto, M., Stryhn, A., Ashmun, R.A., Shapiro, L.H., Arap, W., and Ruoslahti, E. (2000). Aminopeptidase N is a receptor for tumor-homing peptides and a target for inhibiting angiogenesis. Cancer Res. *60*, 722–727.
26. Marchiò, S., Lahdenranta, J., Schlingemann, R.O., Valdembri, D., Wesseling, P., Arap, M.A., Hajitou, A., Ozawa, M.G., Trepel, M., Giordano, R.J., et al. (2004). Aminopeptidase A is a functional target in angiogenic blood vessels. Cancer Cell *5*, 151–162.
27. Arap, W., Kolonin, M., Trepel, M., Cardó-Vila, M., Lahdenranta, J., Giordano, R.J., Mintz, P.J., Ardelt, P.U., Yao, V.J., Vidal, C.I., et al. (2002). Steps toward mapping the human vasculature by phage display. Nat. Med. *8*, 121–127.
28. Fairbrother, W.J., Champe, M.A., Christinger, H.W., Keyt, B.A., and Starovasnik, M.A. (1998). Solution structure of the heparin-binding domain of vascular endothelial growth factor. Structure *6*, 637–648.
29. Ferrara, N., Hillan, K.J., Gerber, H.P., and Novotny, W. (2004). Discovery and development of bevacizumab, an anti-VEGF antibody for treating cancer. Nat. Rev. Drug Discov. *3*, 391–400.
30. Yang, J.C., Haworth, L., Sherry, R.M., Hwu, P., Schwartzentruber, D.J., Topalian, S.L., Steinberg, S.M., Chen, H.X., and Rosenberg, S.A. (2003). A randomized trial of bevacizumab, an anti-vascular endothelial growth factor antibody, for metastatic renal cancer. N. Engl. J. Med. *349*, 427–434.

31. Piotto, M., Saudek, V., and Sklenar, V. (1992). Gradient-tailored excitation for single-quantum NMR spectroscopy of aqueous solutions. J. Biomol. NMR *2*, 661–665.

32. Sklenar, V., Piotto, M., Leppik, R., and Sandek, V. (1993). Gradient-tailored water suppression for 1H–15N HSQC experiments optimized to retain full sensitivity. J. Magn. Reson. A *102*, 241–245.

33. Bax, A., and Davis, D.G. (1985). MLEV-17-based two-dimensional homonuclear magnetization transfer spectroscopy. J. Magn. Reson. *65*, 355–360.

34. Guex, N., and Peitsch, M.C. (1997). SWISS-MODEL and the Swiss-PdbViewer: an environment for comparative protein modelling. Electrophoresis *18*, 2714–2723.